

# PASSIVE ASYMMETRIC TRANSPORT THROUGH BIOLOGICAL MEMBRANES

JEROME S. SCHULTZ

*From the Department of Chemical Engineering, The University of Michigan,  
Ann Arbor, Michigan*

**ABSTRACT** The magnitude of passive diffusional solute transfer through artificial membranes is usually considered to be independent of the direction of the concentration gradient driving force. It can be shown, however, that a composite membrane, having as one component a membrane with a chemical reaction-facilitated diffusion transport mechanism, can result in an asymmetrical flux. An asymmetric flux caused by this type of structural heterogeneity may be one mechanism contributing to the asymmetric properties of biological membranes. Similar vectorial fluxes can be generated in interfacial solute transfer through membranes if hydrodynamic boundary layers occur at the membrane interface and reversible chemical reactions with the permeant species are involved in either phase.

## INTRODUCTION

There have been many reports in the biological literature which have experimentally indicated the existence of passive asymmetric transport phenomena. Asymmetric properties were evidenced by the preferential transport of some species through the membrane in one direction over the opposite direction even at the same concentration gradients of the permeant.

The passive asymmetric flux behavior that we are focusing our attention on here is to be distinguished from "active transport" asymmetric fluxes, where accumulation or concentration of permeants occurs, but coupled to some energetic metabolic reaction and accompanied by a continual consumption of substrate(s). In active transport a net unidirectional flux of a permeant is produced even if the concentration of this solute is initially the same on both sides of the membrane, whereas in passive transport, the condition of equal concentrations or chemical potentials across the membrane is the final equilibrium state, after which no further net transport occurs. The term "passive" as used here is not meant to imply simple Fickian diffusion, but rather to include carrier-mediated transport mechanisms.

Experimental conditions for testing for the existence of passive asymmetric transport in biological systems often cannot be achieved because of the character of the particular system. For example, in a very thorough study of facilitated transport

in erythrocytes, Miller (1) states that the direct uptake of sugars into sugar-free cells could not be accurately measured, and therefore he resorted to tracer techniques to estimate these rates.

In spite of this problem, purely passive asymmetric transport behavior has been experimentally demonstrated. Examples are the studies reported by Narahara and Özand (2) for animal tissues (3-methyl-glucose penetration in frog muscle) and Winkler and Wilson (3) for microbial cells ( $\beta$ -galactoside transport in mutants of *Escherichia coli*). These authors analyzed their data in terms of carrier transport theory, and found  $V_{\max}$  and  $K_m$  were different for influx and efflux experiments.

It should be remarked that Rosenberg and Wilbrandt (4), in their classical paper on facilitated transport, indicated that a "kinetical asymmetry" could be responsible for such behavior. They went as far as to say that a difference in influx and efflux rates with the same concentration gradients was evidence for the existence of chemical reactions in the film.<sup>1</sup> They suggested that a kinetical asymmetry could be the result of different kinetic constants of the carrier-substrate reaction between both sides of the membrane. Although there is precedent for reaction rate constants to change with temperature, ionic strength, and dielectric properties of the solvent there is no direct evidence that such inhomogeneities actually occur in membranes. An equally acceptable hypothesis presented herein, and perhaps more attractive, does not require a variability in reaction rates within a membrane, but rather is based more on structural anisotropic membrane properties.

### STRUCTURAL ANISOTROPY

Several mechanisms based on anisotropic diffusion pathways will be presented in this paper which can be responsible for passive asymmetric transport. That these mechanisms might also be operative in active transport cannot be established at present and is outside the scope of this communication; but Winkler and Wilson's (3) work showed that the same transport system seemed to be responsible for both active and passive  $\beta$ -galactoside penetration, and Schultz (5) has implicated a similar relationship between active and passive transport of sodium and alanine across the brush border of the intestine. By analogy one can expect that if the anisotropic membrane properties postulated here are experimentally confirmed for passive transport, then they may also play a role in active transport. (See *Note Added in Proof*.)

Hartley (6) has pointed out that if the diffusion coefficient of a species is not either independent of its concentration or position in a membrane then it is to be expected that the steady-state flux of this species across a membrane will be asymmetric. An experimental verification of this phenomenon was given by Rogers et al. (7, 8) and

---

<sup>1</sup> This statement cannot be generally correct, in view of the results of Rogers et al. (7) where asymmetric fluxes were demonstrated for simple plastic films.

Stannett (9), who showed that the required dependence of diffusivity on concentration and position could be achieved by placing two plastic membranes in series, at least one of which has the property that the permeability is nonlinear with respect to concentration gradient, or by creating structural anisotropy in a single membrane by chemical or physical means.

Direct evidence for flux asymmetry across a biological membrane has been provided in a recent study by De Bruyne and Van Steveninck (10) on the influx and efflux of dimethyl sulfoxide in yeast under a variety of conditions. They have unequivocally demonstrated that for this substance efflux from the cells is greater than influx. The exact mechanism responsible for the flux asymmetry is not known, and although the kinetics of dimethyl sulfoxide transport is reported as apparently first order, an unequal final distribution of solute between the cell and medium throws some doubt on the presumption that only simple diffusion and no carrier mechanisms are involved.

A somewhat more general mathematical statement than Hartley's for asymmetry of penetration is given by the condition that if  $P_{\text{eff}}$  is not expressible as  $f_x(x) \cdot f_s(S)$ , where  $P_{\text{eff}}$  is the effective permeability of a permeant,  $x$  is position in the membrane, and  $S$  is permeant concentration in the membrane, then asymmetry of transport is to be expected. We have specified  $P_{\text{eff}}$  rather than the diffusivity  $D$  because for many biological membranes a true diffusion coefficient for the permeant in the membrane may not be applicable, as the transport may involve reaction and carrier intermediates. Also, the fraction of membrane area available for transport and the tortuosity of the penetration pathway is usually unknown. There may be situations where penetrant permeability is a joint function of position and concentration, i.e.  $P_{\text{eff}} = f(x, S) \neq f_x(x)f_s(S)$ , and yet symmetric transport prevails. For example, if the membrane is not homogeneous with respect to the relationship between concentration and permeability, but a geometrical plane of symmetry in the membrane exists, then transport will be symmetrical. As shown below, symmetric transport occurs when the boundary concentrations are such that the integral membrane permeability coefficient is the same, independent of the direction of the concentration driving force.

#### CONDITION FOR STRUCTURAL ASYMMETRIC TRANSPORT

It has not been previously recognized that if the permeant species can react reversibly with a mobile membrane component (carrier transport) then conditions promoting structural as opposed to kinetical asymmetric transport can be established. Consider the typical transport flux vs. concentration driving force curve often obtained in biological systems, as depicted in curve A of Fig. 1.

Here we see that the flux through the membrane is not linearly related to the concentration driving force, so that the effective permeability of the solute in the membrane can be considered to be a function of its concentration. In itself, a non-

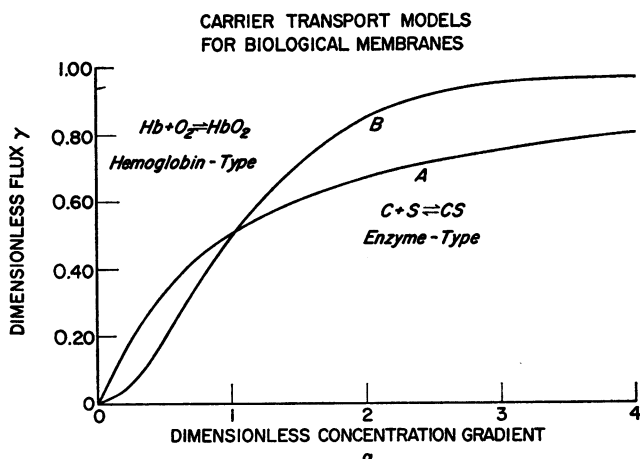


**FIGURE 1** Pattern of facilitated flux across membranes with carrier-type mechanisms which show saturation behavior. Permeant concentration is zero on one side of the membrane.  $\gamma$  = ratio of diffusion flux to maximum flux obtainable.  $\alpha$  = ratio of actual concentration gradient to the gradient which produces one-half of maximum flux.

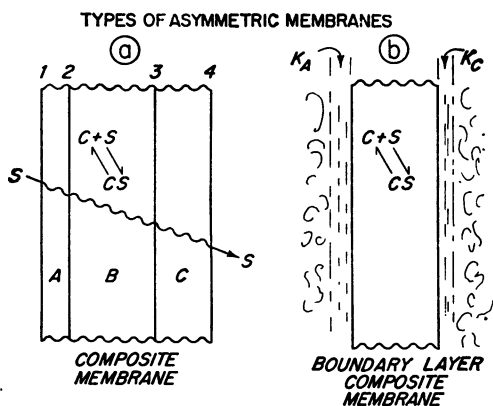


**FIGURE 2** Membrane structural features that can lead to asymmetrical transport. (a) Composite membrane, no reaction in layers A and C, and permeability unequal. Reaction-modulated transport in layer B. (b) Membrane consists only of layer B in which carrier transport can occur. Layers A and C are liquid film resistances.

linear relation between flux and concentration driving force does not lead to asymmetrical mass transport; however, if the diffusion pathway includes another transport resistance in addition to the nonlinear, chemical reaction-modulated step, then a condition can be established where the effective permeability is a joint nonseparable function of position and concentration, a feature which leads to asymmetric mass transport.

Examples of just such membrane structural arrangements are shown in Fig. 2. Fig. 2 a shows a composite membrane consisting of a central core layer in which

reversible transport reactions occur and surface layers where simple Fickian diffusion occurs. If the permeability of the outside layers A and C are unequal, then this is the simplest situation leading to asymmetrical transport. The hydrodynamic boundary layers adjacent to the membrane in Fig. 2 *b* can have simple diffusion behavior similar to the outside membrane layers in Fig. 2 *a* and thus display asymmetric transport. On the other hand, if reversible reactions with the permeant take place in the fluid films A and C, and no reaction occurs in the central layer B, asymmetric transport is again possible. The properties of these structural features that can lead to asymmetric transport are delineated in the development below.

Denoting the permeability of linear diffusion layers A and C by  $P_A$  (cm/sec) and  $P_C$ , and assuming  $P_A > P_C$ , the forward steady-state flux  $J_f$  (moles/cm<sup>2</sup>-sec) through these linear diffusion resistances is given by

$$J_f = P_A(S_1 - S_2) = P_C(S_3 - S_4), \quad (1)$$

where  $S_i$  (moles/cm<sup>3</sup>) is the concentration of permeant at position  $i$ .

For the nonlinear, central layer where  $P_{eff}$  is the effective permeability of the reaction layer<sup>2</sup>

$$J_f = - \int_{S_2}^{S_3} P_{eff} dS. \quad (2)$$

For simplicity, in this development the distribution coefficients of permeant in layers A, B, and C relative to the solvent phase have been assumed to be equal. Substituting equation 1 into the limits of equation 2 gives

$$J_f = - \int_{S_1 - J_f/P_A}^{S_4 + J_f/P_C} P_{eff} dS. \quad (3)$$

Now if the concentration gradient of permeant is reversed, the flux obtained will be given by

$$J_r = P_A(S_1' - S_2') = P_C(S_3' - S_4'), \quad (4)$$

$$J_r = - \int_{S_2'}^{S_3'} P_{eff} dS, \quad (5)$$

where the primes indicate new interfacial compositions. The reversal of concentration gradient can be expressed as

$$S_1' = S_4 \quad \text{and} \quad S_4' = S_1, \quad (6)$$

<sup>2</sup> If the effective permeability of the central membrane layer is a single-valued function of the local activity or concentration so that if expressions of the type  $P_{eff} = f(S)$  can be written. This will only be true for a few special cases where the chemical reaction is fast enough to be considered to be at equilibrium and also the diffusivities of the free carrier and carrier-permeant complex are equal (Bassett and Schultz, 11; Wyman, 12).

so that the limits in equation 5 can be changed by use of equations 4 and 6 to give

$$J_r = - \int_{S_4 - J_r/P_A}^{S_1 + J_r/P_C} P_{\text{eff}} dS. \quad (7)$$

If the magnitudes of forward and reverse fluxes are to be equal, i.e.  $J_f = -J_r = J$ , then the values of the integrals in equations 3 and 7 must be the same, i.e.

$$\int_{S_1 - J/P_A}^{S_4 + J/P_C} P_{\text{eff}} dS = \int_{S_1 - J/P_C}^{S_4 + J/P_A} P_{\text{eff}} dS, \quad (8)$$

or the following equation must be satisfied:

$$\int_{S_4 + J/P_A}^{S_4 + J/P_C} P_{\text{eff}} dS = \int_{S_1 - J/P_C}^{S_1 - J/P_A} P_{\text{eff}} dS. \quad (9)$$

The areas equivalent to the integrals in equation 9 are shown graphically in Fig. 3. In general these integrals will not be equal unless the function  $P_{\text{eff}}$  has the same value at the interfacial solute concentrations, in the region of integral limits, or if  $P_{\text{eff}}$  is a constant independent of the permeant concentration. Therefore, if  $P_{\text{eff}}$  is a function of  $S$  in the central layer B as originally supposed, and  $P_A \neq P_C$ , then the forward and reverse fluxes must be unequal. A composite membrane, consisting only of two membrane layers like A and B, will always show asymmetric flux properties over some range of substrate concentration.

The general features of the composite membrane shown in Fig. 2 a, insofar as diffusion is concerned, are shared by the single membrane and hydrodynamic boundary layers depicted in Fig. 2 b. Here, diffusion through the boundary layers A and C

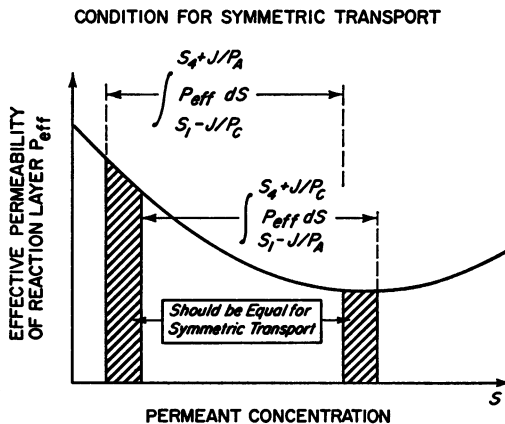


FIGURE 3 Integral conditions that must be satisfied if the fluxes in each direction across a composite are to be equal. In general the shaded areas will not be equal and therefore the flux will be asymmetric.

is linearly related to the concentration gradient from the bulk of the liquid to the membrane interface. Diffusion fluxes through the boundary layers are usually described in terms of mass transfer coefficients, which in turn are a function of flow rates in the region of membrane surface. Thus the apparent permeability of the boundary layers can be altered and controlled by changes in flow rate in the region of the membrane surface and simultaneously affect the asymmetric diffusion properties of the membrane.

#### ANALYTICAL CALCULATION OF ASYMMETRIC TRANSPORT

A general equation which predicts the ratio of forward to reverse flux for a composite membrane system cannot be written because diffusion fluxes through a film with simultaneous chemical reactions cannot generally be expressed in explicit algebraic forms (11, 12); however, some estimate of the magnitude of flux asymmetry that may be developed can be obtained by numerical examples.

Consider a membrane structure consisting of only two layers with the properties of sublayers A and B mentioned above.

If the carrier transport system in the reaction-modulated transport membrane is described by simple symmetric LeFevre enzyme-type kinetics, then for layer B,

$$J_f = V \left[ \frac{S_2}{K_m + S_2} - \frac{S_3}{K_m + S_3} \right]. \quad (10)$$

In terms of this model, the effective permeability of the facilitated transport layer can be expressed as

$$P_{\text{eff}} = \frac{V}{K_m \left( 1 + \frac{S}{K_m} \right)^2}. \quad (11)$$

Also, the flux through the linear transport resistance, layer A, is given by

$$J_f = P_A(S_1 - S_2). \quad (12)$$

since the flux through both membranes must be equal in the steady state, the resultant flux through the membrane composite as a function of the external concentration gradient can be derived by equating equations 10 and 12, solving for  $S_2$ , and substituting this value back into either equation.

$$J_f = \frac{V(S_1 - J_f/P_A)}{K_m + (S_1 - J_f/P_A)} - \frac{VS_3}{K_m + S_3}. \quad (13)$$

Now consider the situation when the concentration gradient across the composite membrane is reversed, then the following equations are obtained:

$$J_r = V \left( \frac{S_1}{K_m + S_1} - \frac{S_2}{K_m + S_2} \right) = P_A(S_2 - S_3), \quad (14)$$

and similar reworking of these equations yields

$$J_r = V \left( \frac{S_1}{K_m + S_1} - \frac{J_r/P_A + S_3}{K_m + J_r/P_A + S_3} \right). \quad (15)$$

The subscript  $f$  denotes that the linear layer is on the side of the membrane sandwich that is exposed to the high substrate concentration, and the subscript  $r$  is for the opposite situation.

The effect of membrane properties and concentration gradients on the asymmetry of transport can be seen more directly if the flux equations are expressed in terms of normalized or nondimensional variables. A reference flux, concentration, and permeability are required to rewrite the equations in normalized form. A convenient set of reference quantities for these variables is as follows:

(a) Reference flux: maximum flux across the carrier transport layer, i.e.,  $V$  for the model represented by equation 10.

(b) Reference concentration: substrate concentration at which flux across the carrier transport layer is one-half the maximum flux, i.e.,  $K_m$ .

(c) Reference permeability: apparent permeability of carrier transport layer (flux/concentration gradient) when the flux across this layer is one-half its maximal value, i.e.,  $(V/2)/K_m$ .

To normalize equations 13 and 15 for the conditions of maximum flux, let  $S_3 = 0$  and substitute the following dimensionless parameters:

(a) Dimensionless concentration = solute concentration/reference concentration:

$$\alpha = S_1/K_m.$$

(b) Dimensionless permeability of linear membrane = permeability/reference permeability:

$$\beta = P_A/(V/2K_m).$$

(c) Dimensionless flux through composite membrane = actual flux/reference flux:

$$\gamma = J/V.$$

When these new variables are substituted into equations 13 and 15, normalized flux equations are obtained (see Appendix).

$$\gamma_f = \frac{\left[ \alpha - \frac{2\gamma_f}{\beta} \right]}{\left[ 1 + \alpha - \frac{2\gamma_f}{\beta} \right]}; \quad \gamma_r = \frac{\alpha}{1 + \alpha} - \frac{2\gamma_r}{\beta + 2\gamma_r}. \quad (16)$$

The quotient  $\gamma_f/\gamma_r$  is a measure of the flux asymmetry since it gives the maximum



ratio of the "forward" to "reverse" fluxes for the same driving force. The terminology "forward" and "reverse" fluxes used here is not meant to imply a direct relation to "influx" and "efflux" for in vivo systems; i.e., the linear diffusion resistance is not necessarily on the external surface of the membrane composite. The flux asymmetry is given by

$$\frac{\gamma_f}{\gamma_r} = \frac{\left\{ \left( \frac{2}{\beta} + \alpha + 1 \right) - \left[ \left( \frac{2}{\beta} + \alpha + 1 \right)^2 - \frac{8\alpha}{\beta} \right]^{1/2} \right\} (1 + \alpha)}{- \left( \frac{2}{\beta} + \alpha + 1 \right) + \left[ \left( \frac{2}{\beta} + \alpha + 1 \right)^2 + \frac{8\alpha(1 + \alpha)}{\beta} \right]^{1/2}}; \quad (17)$$

The ratio of the maximum forward to reverse fluxes ( $\gamma_f/\gamma_r$ ) is shown in Fig. 4 as a function of the dimensionless concentration gradient  $\alpha$ , with the permeability  $\beta$  of the linear layer as a parameter. Over the range of variables portrayed, the asymmetry of the membrane composite increases with higher concentration gradients and lower permeability of the linear layer. At low concentration gradients flux asymmetry is minimal over wide ranges of  $\beta$ . This behavior is because of the fact that, when exposed to low concentration gradients, the flux characteristics of the reaction-modulated layer approaches linearity.

The dimensionless flux through the composite membrane, in the forward and reverse directions, for three values of the permeability of the linear membrane layer, is plotted as a function of the concentration gradient in Fig. 5. The appearance of this graph is similar to those often measured in biological transport studies when the

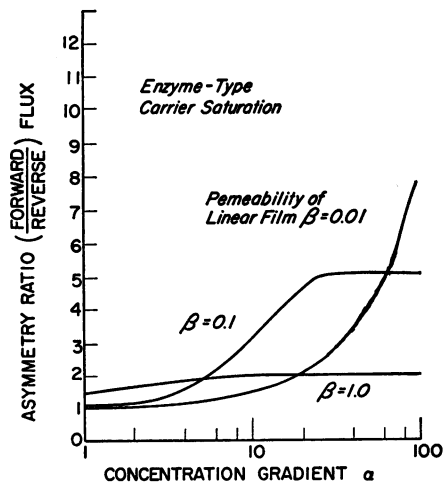


FIGURE 4 Asymmetric flux calculated for a two-membrane system, one membrane with enzyme-type transport characteristics (curve A, Fig. 1), and the other obeying linear transport.  $\beta$  is the permeability of the linear transport layer divided by the effective permeability of the carrier transport layer when the concentration gradient  $\alpha = 1$ .

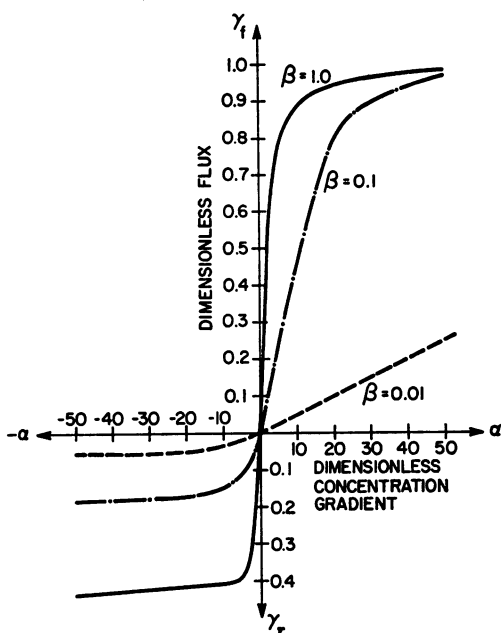


FIGURE 5 The forward ( $\gamma_f$ ) and reverse ( $\gamma_r$ ) fluxes through a composite reaction-modulated membrane as a function of the direction and magnitude of the applied concentration gradient  $\alpha$ . Parameter  $\beta$  is the dimensionless permeability of the linear (nonreactive) layer. Note that for low values of  $\alpha$ , the forward flux ( $\gamma_f$ ) is linear with increasing concentration but the reverse flux ( $\gamma_r$ ) shows saturation characteristics.

concentration of permeant is kept at 0 on one side of the membrane. The composite membrane still shows saturation characteristics with respect to substrate concentration as does a single membrane with carrier-facilitated diffusion.

The format of this graph, to illustrate structural asymmetry, is similar to the format used by Rosenberg and Wilbrandt (4) to show kinetical asymmetry (reproduced here as Fig. 6). The striking similarity of predicted transport behavior for these very different mechanisms indicates that experimental methods to distinguish between these two mechanisms for biological membranes will need to be extremely precise.

If a Lineweaver-Burk-type plot is made for the calculated transport rates across the composite film ( $\beta = 0.1$ ) some nonlinearity is apparent near the origin in Fig. 7 (solid lines). This deviation from linearity might be used as a diagnostic characteristic to infer whether a natural membrane can be modeled as a composite structure, but the accuracy and reproducibility of experimental transport rates are usually not good enough to determine these curves accurately. Based on this plot (dashed lines) estimates of the carrier model constants are  $V = 1$  and  $K_m = 11\alpha$  for the forward transport process, and  $V = 0.20$  and  $K_m = 3\alpha$  for the reverse transport process. These apparent facilitation kinetic constants are to be contrasted with the assumed

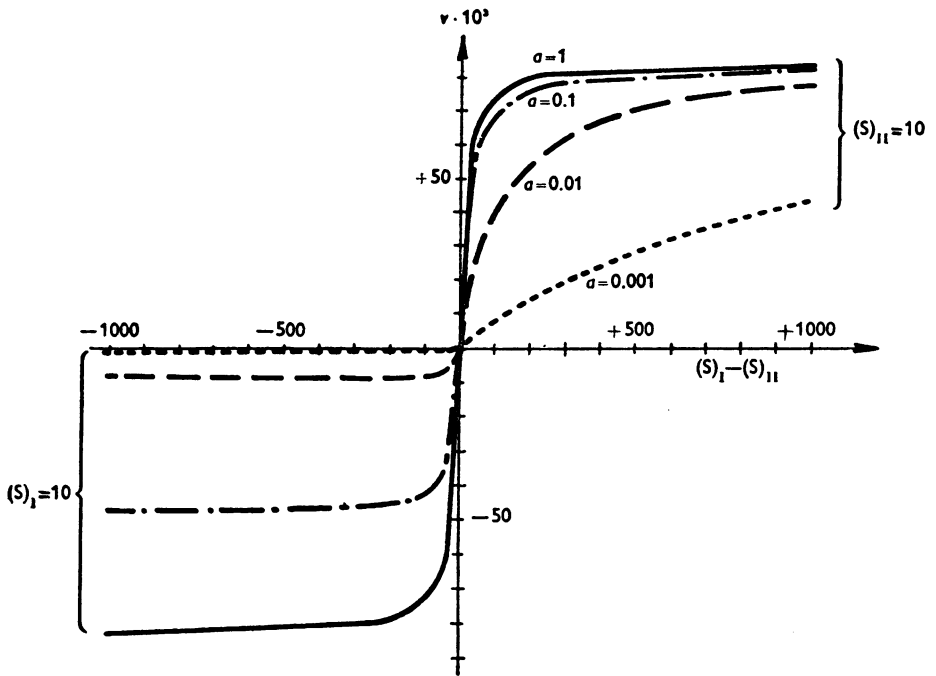


FIGURE 6 Kinetical asymmetry of the nonenzymatic carrier transport reproduced from Rosenberg and Wilbrandt (4). Ordinate: rate of transport. Abscissa: concentration difference across membrane. Parameter  $a$  is velocity constant for the reaction of solute with free carrier on one side of the membrane. In plotting this figure the same velocity constant on the other side of the membrane was assumed to have a value of 1.0. (Fig. 5 of Rosenberg, T., and W. Wilbrandt. 1955. *Exp. Cell Res.* 9:49. Copyright held by Academic Press, Inc., New York.)

values of  $V = 1$  and  $K_m = 1\alpha$  used earlier as model constants in these example calculations to characterize the carrier-modulated transport layer.

The need for a diagnostic theoretical and experimental approach to distinguish between the kinetic and structural models for asymmetric transport seems evident. Processing experimental data either as displayed in Figs. 5 and 6 or as in Fig. 7 would not seem sensitive enough to infer which model was more appropriate for a particular experimental circumstance. Another approach is to develop a method for plotting experimental data so as to be able to differentiate easily between kinetic and structural models. Although there is no generally accepted model for the kinetics of membrane transport, the kinetic equations given by Regen and Morgan (13) cover many of the mechanisms that have been advanced for carrier transport and will be used here to contrast with the composite membrane model. These equations can be manipulated (see Appendix) to arrive at a format in which the experimental data should plot as a straight line if the kinetical model is applicable, i.e.

$$\frac{1}{S_1} \left( \frac{J_f}{J_i} - 1 \right) = A - B \frac{J_f}{J_r} \text{ or } \frac{1}{\alpha} \left( \frac{\gamma_f}{\gamma_r} - 1 \right) = AK_m - BK_m \frac{\gamma_f}{\gamma_r}, \quad (18)$$

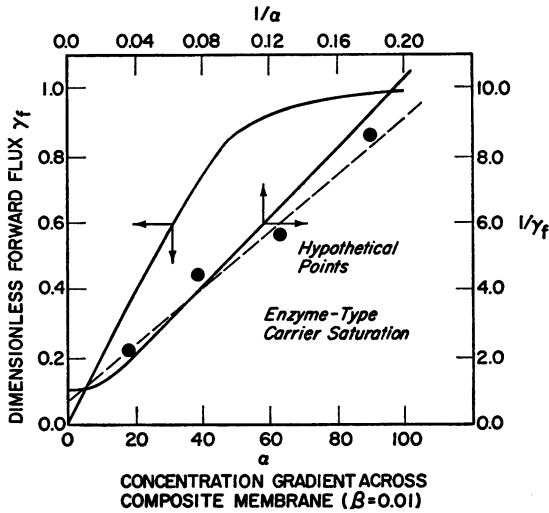


FIGURE 7 Dimensionless flux through composite membrane in the direction from linear to nonlinear layer as a function of concentration gradient (left-hand scale). Lineweaver-Burk plot of transport rate (right-hand scale); solid line, theoretical curve; dashed line, hypothetical experimental results.

where  $J_f$  and  $J_r$  are the maximum values of the forward and reverse unidirectional fluxes at the same value of concentration gradient, i.e., with the permeant concentration equal to zero on one side of the membrane.

The constants  $A$  and  $B$  which can be obtained from the slope and intercept of the line, are related to the kinetic constants by

$$A = 1/K_{s_i}, \quad B = 1/K_{s_o}$$

for Regen and Morgan's model, and

$$A = \frac{1}{K \left[ 1 + \frac{ad}{b(a+D)} \right]}, \quad B = \frac{1}{K \left[ 1 + \frac{bD}{a(b+D)} \right]}$$

for Rosenberg and Wilbrandt's model of kinetical asymmetry.

Many of the carrier transport models, such as proposed by Rosenberg and Wilbrandt (4) and Levine and Stein (14), are but special cases of Regen and Morgan's formulations. If membrane transport for a particular system is describable by any of these kinetic models then a plot of the forward and reverse fluxes should also appear as straight lines with the coordinates shown.

If asymmetry in diffusive flux is a result of *structural* anisotropy, however, then when the data is plotted using the same coordinate systems as indicated in Fig. 8, a straight line will not usually result. Hypothetical calculated data for asymmetric transport fluxes shown in Fig. 5 for structural asymmetry give very nonlinear curves

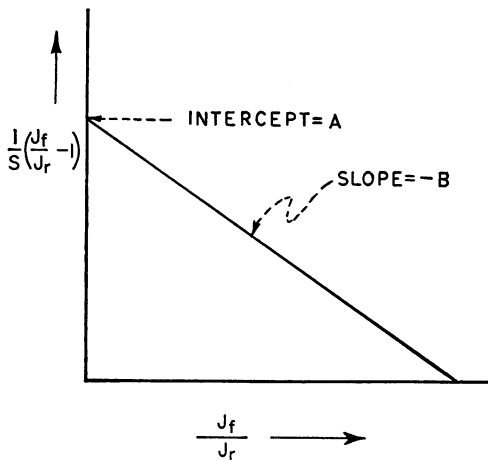


FIGURE 8

FIGURE 8 A method of plotting data on fluxes through membranes to distinguish between kinetic and structural models for asymmetric transport. The kinetic model equations can be put into the form

$$\frac{1}{S} \left( \frac{J_f}{J_r} - 1 \right) = A - B \left( \frac{J_f}{J_r} \right).$$

Data following this model would follow a straight line on the coordinates shown here. If flux data on a particular membrane do not plot as a straight line on these coordinates, then it is unlikely that the kinetic model is a valid description of that membrane transport system.

FIGURE 9 A plot, according to the coordinates of Fig. 8, of the flux through a hypothetical membrane in which there is both structural asymmetry and carrier transport. The curve given here is equivalent to the curves labeled  $\beta = 0.1$  in Figs. 4 and 5, and shows extreme nonlinearity when plotted according to these coordinates.

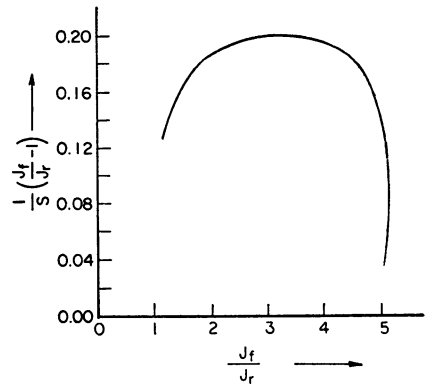


FIGURE 9

when plotted according to the coordinates indicated by equation 18 (Fig. 9). If membrane flux data do not plot linearly on these coordinates, then this evidence implies that other than purely kinetical explanations for the transport process need to be invoked. Unfortunately, the type of plot illustrated by Fig. 8 is not useful for the determination of the model constants for structural asymmetric transport, and other approaches would be required to completely characterize membrane properties.

### GRAPHICAL CALCULATION OF ASYMMETRICAL TRANSPORT

If the carrier transport system in the composite membrane has the kinetic characteristics of the hemoglobin saturation curve in Fig. 1 (curve B), then similar asymmetric flux characteristics as a function of the dimensionless concentration gradient  $\alpha$  and permeability of the linear layer  $\beta$  are predicted (Fig. 10). The fluxes for these illustrations were calculated by the graphical methods given in the Appendix. The maximum asymmetric flux ratio obtained is greatest with sigmoid type saturation

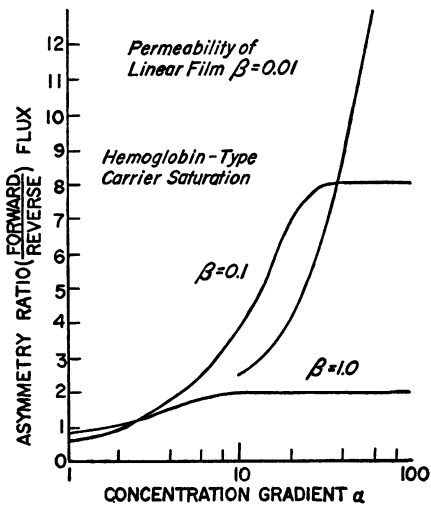


FIGURE 10

FIGURE 10 Asymmetric flux calculated for a two-membrane system, one membrane with hemoglobin-type transport characteristics (curve B, Fig. 1), and the other obeying linear transport.

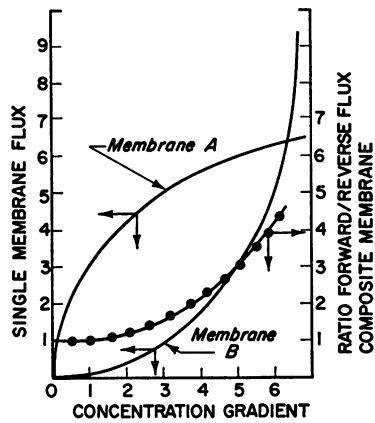


FIGURE 11

FIGURE 11 Asymmetric flux produced by two nonlinear transport layers in series.

kinetics as illustrated by the hemoglobin system. This case is also interesting because the direction of asymmetry changes over a range of concentration gradients. At low concentrations the flux is higher when the carrier layer is exposed to zero permeant concentration, whereas at high concentration gradients the flux is higher when the carrier layer is on the side with no permeant. There is a particular concentration gradient ( $\alpha \cong 3$ ) where no asymmetry is developed.

Direct evidence for an asymmetric flux in this type of system has been given by Scholander (15). He found that the ratio of oxygen to nitrogen transport, through a membrane composite consisting of a hemoglobin layer and a water layer, was a function of the direction of the applied concentration gradient. In this case, nitrogen does not react with the hemoglobin carrier and therefore is not subject to an asymmetric flux, whereas oxygen does react and is transported asymmetrically.

Of course if both membrane layers have nonlinear flux characteristics (for a hypothetical example see Fig. 11), then the composite will usually also have asymmetric transport behavior. These transport rates cannot be nondimensionalized in the same fashion as the previous examples, but the ratio of forward to reverse fluxes as a function of concentration gradient can be very substantial as seen by the dotted curve in Fig. 11.

## DISCUSSION

Whether the mechanism of asymmetric transport as a result of membranes with composite structures and nonlinear carrier-mediated transport characteristics can

contribute to the explanation of asymmetric biological transport phenomena as sugar transport in bacteria (2), sugar transport in muscles (3), dimethyl sulfoxide transport in yeast (10), and unequal sugar fluxes into and out of erythrocytes (1) will have to await further experimentation designed to test this composite membrane theory; but there can be no doubt that the asymmetric transport behavior of nonlinear composite layers will have some influence on transport in biological systems, and therefore experiments should be designed to estimate the role of these factors in the membrane transport properties.

There are a few observations with biological membranes which might be better understood in terms of the composite membrane model described here. For instance several workers have noted that permeation rates are saturable in one direction of transport but are first order in the opposite direction (e.g., Koch [16]). The latter process is often termed a "leak." Curves in Fig. 5 show that in the range of concentration up to  $\pm 20\alpha$ , that the reverse transport rate  $\gamma_r$  appears to saturate while the forward rate appears to follow linear kinetics.

Also, while many simultaneous facilitated transport processes in the same membrane appear to be very specific for individual solutes, agents as hormones, e.g. insulin and vasopressin (17), seem to affect several solute transport rates simultaneously. This could be rationalized by postulating that the hormone changed the permeability of a "linear" layer which all solutes must penetrate rather than interacting with each of the specific carrier transporters. Hays and Franki (18) have demonstrated just such an effect in the action of vasopressin on the rate of water diffusion through toad bladder membranes. Both the epithelial and supporting layers of the bladder wall contribute to the diffusion resistance of water, but in changing water transport rates, vasopressin is thought to act primarily on the epithelial layer. Their "dual-barrier" hypothesis can be viewed as an example of a structural anisotropic membrane proposed in this paper.

In addition, Hays and Franki give data showing that stirring the solutions adjacent to the membrane in *in vitro* experiments could dramatically affect transport rates. This is evidence for the hydrodynamic boundary layers as depicted in Fig. 2 *b*, and leads to the possibility that asymmetrical transport rates may be demonstrated in *in vitro* studies with carrier transport membranes but caused by an artifact of unequal boundary layer resistances.

This work was supported by the National Institutes of Health, grant number GM-15152, and a Research Career Development Award (No. 1K04GM08271-01) from the institute of General Medical Sciences.

*Received for publication 19 February 1970 and in revised form 5 January 1971.*

*Note Added in Proof.* F. Sauer (Max Planck Institut für Biophysik) has proved by irreversible thermodynamics that a necessary condition for active asymmetric transport across membranes is a membrane structure which can produce passive asymmetric transport. (Symposium on Passive Permeability of Cell Membranes, Rotterdam, July 20, 1971).

## REFERENCES

1. MILLER, D. M. 1968. *Biophys. J.* **8**:1329.
2. NARAHARA, H. T., and P. ÖZAND. 1963. *J. Biol. Chem.* **238**:40.
3. WINKLER, H. H., and T. H. WILSON. 1966. *J. Biol. Chem.* **241**:2200.
4. ROSENBERG, T., and W. WILBRANDT. 1955. *Exp. Cell Res.* **9**:49.
5. SCHULTZ, G. S. 1969. In *Biological Membranes*. R. M. Dowben, editor. Little, Brown and Company, Boston. 59.
6. HARTLEY, G. S. 1948. *Discuss. Faraday Soc.* **3**:223.
7. ROGERS, C. E., V. STANNETT, and M. SWARC. 1957. *Ind. Eng. Chem.* **49**:1933.
8. ROGERS, C. E. 1965. *J. Polym. Sci. Part C.* **10**:93.
9. STANNETT, V., J. L. WILLIAMS, A. B. GOSNELL, and J. A. GERVASI. 1968. *J. Polym. Sci. Part B.* **6**:185.
10. DE BRUYNE, A. W., and J. VAN STEVENINCK. 1970. *Biochim. Biophys. Acta.* **211**:555.
11. BASSETT, J., and J. S. SCHULTZ. 1970. *Biochim. Biophys. Acta.* **211**:194.
12. WYMAN, J. 1966. *J. Biol. Chem.* **241**:115.
13. REGEN, D. M., and H. E. MORGAN. 1964. *Biochim. Biophys. Acta.* **79**:151.
14. LEVINE, M., and W. A. STEIN. 1966. *Biochim. Biophys. Acta.* **127**:179.
15. SCHOLANDER, P. F. 1965. *Science (Washington)*. **149**:876.
16. KOCH, A. L. 1967. *J. Theor. Biol.* **14**:102.
17. LICHTENSTEIN, N. S., and A. LEAF. 1966. *Ann. N.Y. Acad. Sci.* **137**:556.
18. HAYS, R. M., AND N. FRANKI. 1970. *J. Membrane Biol.* **2**:263.

## APPENDIX

### *Normalization of Membrane Transport Equations*

The forward flux equation for the maximum transport rate across a carrier membrane composite is (from equation 13 and  $S_3 = 0$ )

$$J_f = \frac{V(S_1 - J_f/P_A)}{K_m + (S_1 - J_f/P_A)}. \quad (\text{A } 1)$$

This equation can be rearranged to

$$\frac{J_f}{V} = \frac{\left[ \frac{S_1}{K_m} - \frac{J_f}{V} \frac{V}{P_A K_m} \right]}{\left[ 1 + \frac{S_1}{K_m} - \frac{J_f}{V} \frac{V}{P_A K_m} \right]}, \quad (\text{A } 2)$$

and making the substitutions  $\alpha = S_1/K_m$ ,  $\beta = 2K_m P_A/V$ , and  $\gamma_f = J_f/V$ , one obtains

$$\gamma_f = \frac{\left[ \alpha - \frac{2\gamma_f}{\beta} \right]}{\left[ 1 + \alpha - \frac{2\gamma_f}{\beta} \right]}. \quad (\text{A } 3)$$

Similarly, to find the normalized equation for the maximum reverse flux, (from equation 15,  $S_3 = 0$ )

$$J_r = V \left( \frac{S_1}{K_m + S_1} - \frac{J_r/P_A}{K_m + J_r/P_A} \right), \quad (\text{A } 4)$$



which can be rearranged to

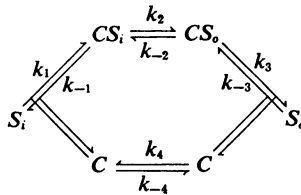
$$\frac{J_r}{V} = \left[ \frac{\frac{S_1}{K_m}}{1 + \frac{S_1}{K_m}} - \frac{\frac{J_r}{V}}{\frac{K_m P_A}{V} - \frac{J_r}{V}} \right], \quad (\text{A } 5)$$

and, making the substitutions indicated above, one obtains

$$\gamma_r = \frac{\alpha}{1 + \alpha} - \frac{\gamma_r}{(\beta/2) + \gamma_r}. \quad (\text{A } 6)$$

*Diagnostic Graphical Method for Asymmetric Transport due to Kinetical Asymmetry*

Regen and Morgan gave the following model for carrier transport:



and derived the following equation for unidirectional fluxes.

Flux from right to left (efflux):

$$v_{s-} = \frac{[S_i]F_s}{1 + \frac{[S_i]}{B_s} + \frac{([S_i] - [S_o])M_{SI}}{1 + [S_o]/R_s}} = J_f. \quad (\text{A } 7)$$

Flux from left to right:

$$v_{s+} = \frac{[S_o]F_s}{1 + \frac{[S_o]}{B_s} + \frac{([S_o] - [S_i])M_{So}}{1 + [S_i]/R_s}} = J_r, \quad (\text{A } 8)$$

where  $S_o$  and  $S_i$  refer to substrate concentrations outside the membrane, and the other symbols are related to the kinetic constants. (See reference 18 for exact relationships, kinetic constants, and model constants.)

The maximum unidirectional fluxes are obtained by setting  $S_o$  and  $S_i$  to zero in equations A 7 and A 8 respectively.

$$J_f = \frac{S_o F_s}{1 + S_o \left( \frac{1}{B_s} + M_{S_o} \right)} = \frac{S_o F_s}{1 + S_o / K_{S_o}}, \quad (\text{A } 9)$$

$$J_r = \frac{S_i F_s}{1 + S_i \left( \frac{1}{B_s} + M_{S_i} \right)} = \frac{S_i F_s}{1 + S_i / K_{S_i}}, \quad (\text{A } 10)$$

and the ratio of maximum forward to maximum reverse flux is

$$\frac{J_f}{J_r} = \frac{\frac{S_o F_S}{1 + S_o/K_{S_o}}}{\frac{S_i F_S}{1 + S_i/K_{S_I}}}, \quad (\text{A } 11)$$

at the same concentration gradient, i.e.,  $S_i = S_o = S_1$  (defined in text), this ratio of fluxes becomes

$$\frac{J_f}{J_r} = \frac{1 + (S_1/K_{S_I})}{1 + (S_1/K_{S_o})}. \quad (\text{A } 12)$$

Now this equation can be rearranged.

$$\frac{J_f}{J_r} + \frac{J_f}{J_r} \frac{S_1}{K_{S_o}} = 1 + \frac{S_1}{K_{S_I}}.$$

Collecting terms in  $S_1$  :

$$\frac{J_f}{J_r} - 1 = S_1 \left( \frac{1}{K_{S_I}} - \frac{J_f}{J_r} \frac{1}{K_{S_o}} \right)$$

Dividing by  $S_1$  :

$$\frac{1}{S_1} \left( \frac{J_f}{J_r} - 1 \right) = \frac{1}{K_{S_I}} - \frac{J_f}{J_r} \frac{1}{K_{S_o}} = A - B \frac{J_f}{J_r}. \quad (\text{A } 13)$$

The form given in equation A 13 shows that if transport data on fluxes  $J_f$  and  $J_r$  at various substrate levels ( $S$ ) are plotted as  $(1/S)[(J_f/J_r) - 1]$  vs.  $J_f/J_r$ , then a straight line should result of the form given in Fig. 8.

Rosenberg and Wilbrandt's (4) kinetical asymmetry model is a special case of that shown above, but with the restriction that  $k_2 = k_{-2} = k_4 = k_{-4} = D'$ , where  $D'$  is the diffusivity of the carrier in the membrane. A linearization equivalent to equation A 13 would also be obtained from their equations.

*Graphical Evaluation Diffusion Fluxes.* When fluxes through the individual elements comprising the composite membrane cannot be expressed in an analytical form, one can use graphical techniques to evaluate the net steady flux through the membrane. Let the maximum flux vs. concentration relationship for each of the membrane sections be represented by  $J_A(S)$  and  $J_B(S)$ , where  $J_A(S)$  is defined as the flux that would pass through membrane A if the concentration of permeant was zero on one side and  $S$  on the other. Two example flux vs. concentration curves are shown in Fig. A 1. If for an arbitrary concentration gradient ( $S' - S''$ ) the flux through each of the membrane sections can be represented by

$$J_A = j_A(S') - j_A(S'') \quad (\text{A } 14)$$

$$J_B = j_B(S') - j_B(S'') \quad (\text{A } 15)$$

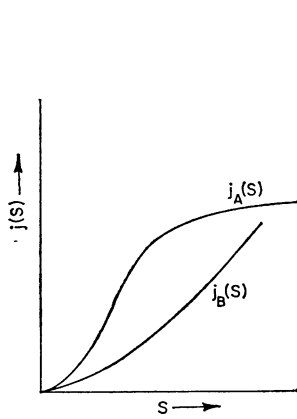


FIGURE A 1

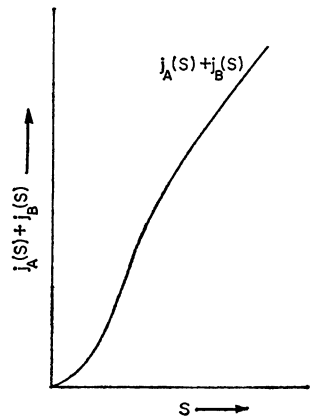


FIGURE A 2

FIGURE A 1 Graphical method for obtaining net flux through a membrane which is composed of two sections with different solute transport characteristics. Hypothetical flux characteristics of individual membrane sections A and B, as a function of solute concentration difference  $S$ . (Solute concentration is  $S$  on one side and zero on the other side of the membrane.)

FIGURE A 2 Graphical method for obtaining net flux through a membrane which is composed of two sections with different solute transport characteristics. Membrane flux function ( $j_A + j_B$ ) as related to solute concentration.

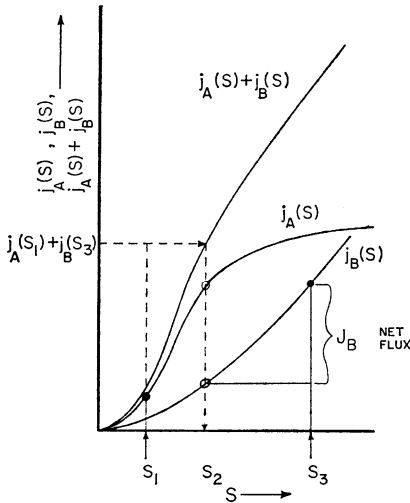


FIGURE A 3

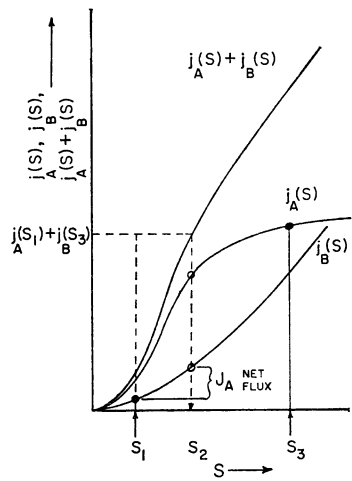


FIGURE A 4

FIGURE A 3 Graphical method for obtaining net flux through a membrane which is composed of two sections with different solute transport characteristics. Graphical determination of net flux  $= J_B$ ; when the A section of a composite membrane is exposed to solute concentration  $S_1$ , and the B section of a membrane is exposed to solute concentration  $S_3$ .  $S_2$  is the calculated concentration of solute at the interface of membrane sections A and B.

FIGURE A 4 Graphical method for obtaining net flux through a membrane which is composed of two sections with different solute transport characteristics. Graphical determination of net flux  $= J_A$ , when the B section of a composite membrane is exposed to solute concentration  $S_1$ , and the A section of a membrane is exposed to solute concentration  $S_3$ .

(See previous footnote concerning this assumption.) Then the net flux can be estimated by the following graphical technique, which is somewhat more general than the method given by Rogers et al. (7). As mentioned in the text, the steady-state flux through each section must be equal, so that

$$J_A = J_B . \quad (\text{A } 16)$$

Also, from the above assumption and using the symbols of the text

$$J_A = j_A(S_2) - j_A(S_1), \quad (\text{A } 17)$$

$$J_B = j_B(S_3) - j_B(S_2), \quad (\text{A } 18)$$

where  $S_1$ ,  $S_2$ , and  $S_3$  are the permeant concentrations at the left face, interface, and right face of the composite membrane.

We then have, equating equations A 17 and A 18

$$j_A(S_2) - j_A(S_1) = j_B(S_3) - j_B(S_2), \quad (\text{A } 19)$$

or, rearranging,

$$j_A(S_1) + j_B(S_3) = j_A(S_2) + j_B(S_2). \quad (\text{A } 20)$$

The right-hand side of this equation involves only a single concentration and can be represented graphically by the sum of functions  $j_A$  and  $j_B$ , Fig. A 2. The curves in Fig. A 2 can be used to solve for the flux through the composite membrane. First equation A 20 is solved graphically to find the interfacial concentration  $S_2$ . Lines or straight edges are put on the figure to find the values of  $j_A(S_1)$  and  $j_B(S_3)$  (see Fig. A 3). Then the sum  $j_A(S_1) + j_B(S_3)$  is plotted at position  $S = S_1$ . This line is projected over to the  $(j_A + j_B)$  curve, and the point of intersection gives the value of  $S_2$ . Now the net flux,  $J_A = J_B$ , is found by evaluating the difference  $j_A(S_2) - j_A(S_1)$  on the  $j_A$  curve, or  $j_B(S_3) - j_B(S_2)$  as shown in Fig. A 3.

If the membrane is reversed with respect to the concentration gradient, i.e. membrane A faces  $S_3$  and membrane B faces  $S_1$ , then the sum  $j_A(S_3) + j_B(S_1)$  is plotted at  $S = S_1$ . Then, as before, this sum is projected to the  $j_A + j_B$  curve to find  $S_2$  (see Fig. A 4), and the net flux,  $J_B = j_B(S_2) - j_B(S_1) = J_A$ , is found from the  $j_B$  curve.